



Identification of patients with acute coronary syndrome and representation of their degree of inflammation: application of pericoronary adipose tissue within different radial distances of the proximal coronary arteries

Xiaolin Dong^{1^}, Chentao Zhu^{1^}, Na Li^{1^}, Ke Shi¹, Nuo Si¹, Yujia Wang², Hong Pan¹, Zhenzhou Shi¹, Shuting Wang¹, Min Zhao³, Tong Zhang^{1^}

¹Department of Radiology, Fourth Affiliated Hospital of Harbin Medical University, Harbin, China; ²Department of Interventional and Vascular, Fourth Affiliated Hospital of Harbin Medical University, Harbin, China; ³Pharmaceutical Diagnostics, GE Healthcare, Beijing, China

Contributions: (I) Conception and design: X Dong, C Zhu, N Li; (II) Administrative support: T Zhang; (III) Provision of study materials or patients: X Dong; (IV) Collection and assembly of data: X Dong, K Shi, N Si, Y Wang, H Pan, Z Shi, S Wang; (V) Data analysis and interpretation: M Zhao; (VI) Manuscript writing: All authors; (VII) Final approval of manuscript: All authors.

Correspondence to: Tong Zhang. Department of Radiology, Fourth Affiliated Hospital of Harbin Medical University, 37 Yiyuan Street, Nangang District, Harbin 150001, China. Email: yingxiang939@163.com.

Background: Pericoronary adipose tissue (PCAT) around the proximal right coronary artery (RCA) is considered a marker of coronary inflammation. We aimed to explore the segments of PCAT that represent coronary inflammation in patients with acute coronary syndrome (ACS) and to identify patients with ACS and stable coronary artery disease (CAD) prior to intervention.

Methods: We retrospectively enrolled consecutive patients with ACS and stable CAD who underwent invasive coronary angiography (ICA) after coronary computed tomography angiography (CCTA) from November 2020 to October 2021 at the Fourth Affiliated Hospital of Harbin Medical University. The fat attenuation index (FAI) was obtained using PCAT quantitative measurement software, and the coronary Gensini score was also calculated to indicate the severity of CAD. The differences and correlations between FAI within different radial distances of proximal coronary arteries were evaluated, and the recognition ability of FAI for patients with ACS and stable CAD was evaluated by establishing receiver operator characteristic (ROC) curves.

Results: A total of 267 patients were included in the cross-sectional study, including 173 patients with ACS. With the increase of radial distance from the outer wall of proximal coronary vessels, the FAI decreased ($P < 0.001$). The FAI around the proximal left anterior descending artery (LAD) within the reference diameter from the outer wall of the vessel (LAD_{ref}) had the highest correlation with the FAI around culprit lesions [$r = 0.587$; 95% confidence interval (CI): 0.489–0.671; $P < 0.001$]. The model based on clinical features, Gensini score, and LAD_{ref} had the highest recognition performance for patients with ACS and stable CAD [area under the curve (AUC): 0.663; 95% CI: 0.540–0.785].

Conclusions: LAD_{ref} is most correlated with FAI around culprit lesions in patients with ACS and has higher value in the preintervention differentiation of patients with ACS and stable CAD compared to the use of clinical features alone.

[^] ORCID: Xiaolin Dong, 0000-0001-9081-2165; Chentao Zhu, 0000-0002-9169-6212; Na Li, 0000-0002-8463-7441; Tong Zhang, 0000-0003-1123-7874.

Keywords: Acute coronary syndrome (ACS); coronary artery disease (CAD); pericoronary adipose tissue (PCAT); fat attenuation index (FAI); coronary computed tomography angiography (CCTA)

Submitted Aug 16, 2022. Accepted for publication Mar 24, 2023. Published online Apr 12, 2023.

doi: 10.21037/qims-22-864

View this article at: <https://dx.doi.org/10.21037/qims-22-864>

Introduction

Coronary artery disease (CAD) is one of the diseases with the highest morbidity in the world (1), and despite current improvements in interventional and pharmacological treatments, acute coronary syndrome (ACS) remains a leading cause of death in developed countries (2). Inflammation of coronary vessels will ultimately promote atherosclerosis and atherothrombosis in patients with ACS (3,4). In recent years, it has been shown that pericoronary adipose tissue (PCAT) plays an important role in the occurrence and development of CAD (5), and PCAT has demonstrated value as a predictor of CAD stratification (6) and cardiac mortality (7). Although intravascular imaging (8) and positron emission tomography-computed tomography (PET-CT) (9) can confirm localized adipose tissue inflammation in culprit lesions, the complexity of the scanning method and high cost limit its clinical use (10); however, standard noninvasive methods cannot monitor coronary inflammation (11). Research has demonstrated that vascular inflammation inhibits the local adipogenesis of PCAT, which enables the noninvasive detection of the fat attenuation index (FAI) in proximal coronary arteries via coronary CT angiography (CCTA) (5).

A previous study showed that PCAT proximal to the right coronary artery (RCA) correlates with coronary inflammation (5). Another study found that the FAI was higher around the left anterior descending artery (LAD) and the left circumflex artery (LCX) than in the RCA (12), indicating a more severe degree of inflammation. In patients with vasospastic angina (VSA), PCAT closer to the vessel wall was found to have a better diagnostic performance for the disease than did PCAT within the reference diameter (13). Moreover, patients with stable CAD and acute myocardial infarction (MI) can be differentiated with PCAT (6). However, when deciding whether patients with CAD should undergo interventional therapy, it is necessary to carefully evaluate its severity to prevent the omission of severe ACS and the over examination of stable CAD. Therefore, this study mainly aimed to determine whether

there is a better site of PCAT that correlates more highly with inflammation at culprit lesions, and whether it is possible to initially identify patients with ACS and stable CAD using PCAT prior to invasive coronary angiography (ICA) examination. We present the following article in accordance with the STROBE reporting checklist (available at <https://qims.amegroups.com/article/view/10.21037/qims-22-864/rc>).

Methods

Participants and study design

This was a retrospective cross-sectional study. The recruitment of patients and the measurement of various parameters were carried out from November 2021 to January 2022. We retrospectively recruited consecutive patients with CAD who were examined and diagnosed in The Fourth Affiliated Hospital of Harbin Medical University from November 2020 to October 2021. These patients underwent CCTA scans after being highly suspected of CAD due to chest pain or changes in electrocardiogram (ECG) dynamics or abnormal laboratory tests during their hospitalization, which was followed by ICA within 48 hours and then diagnosis of ACS or stable CAD by two experienced cardiologists. Finally, 94 patients with stable CAD and 173 patients with ACS were included. Patients with ACS were considered those with unstable angina (UA) (n=150) and ST-segment elevation myocardial infarction (STEMI) or non-ST-segment elevation myocardial infarction (NSTEMI) after thrombolysis (n=23). Our study included major coronary branches with $\geq 25\%$ stenosis in each patient with ACS, where culprit lesions were identified in ICA according to clinical guidelines [specific identification methods shown in Supplementary file (Appendix 1)] (14), and a non-culprit lesion was considered to be most severe lesion of each included vessel. We excluded patients with a history of coronary revascularization or MI, allergy to iodinated contrast agents, poor image quality on CCTA, and

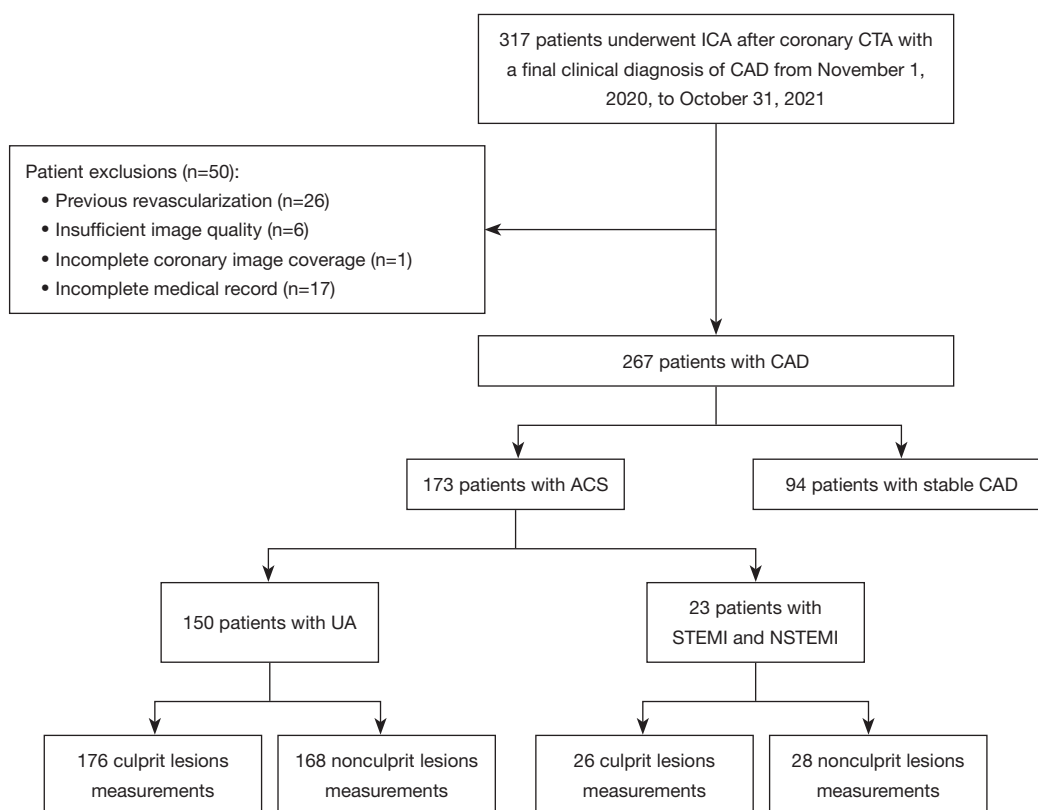


Figure 1 Flowchart showing inclusion and exclusion criteria for the study population. ICA, invasive coronary angiography; CTA, computed tomography angiography; CAD, coronary artery disease; ACS, acute coronary syndrome; UA, unstable angina; STEMI, ST-segment elevation myocardial infarction; NSTEMI, non-ST-segment elevation myocardial infarction.

inadequate coronary imaging coverage. *Figure 1* illustrates the patient inclusion and exclusion criteria. The study was conducted in accordance with the Declaration of Helsinki (as revised in 2013). The study was approved by the Medical Ethics Committee of The Fourth Affiliated Hospital, Harbin Medical University (No. 2022-SCILLSC-13), and individual consent for this retrospective analysis was waived.

Definition of cardiovascular risk factors

All cardiovascular risk factors [Supplementary file (Appendix 1)] of the included cases were obtained from inpatient medical records by a panel of two cardiologists.

CCTA scan protocol

CCTA imaging was performed on a 320-detector row CT scanner (Aquilion ONE; Toshiba, Tokyo, Japan). All patients

with a baseline heart rate >65 beats/min were given beta blockers (metoprolol, 25–75 mg) orally 1 hour before the examination to bring the heart rate down to the standard heart rate and below. A dual-channel high-pressure syringe was used to inject 60–80 mL of nonionic iodine contrast agent (iohexol in injection containing 350 mg/L of iodine; GE Healthcare, Chicago, IL, USA) at a rate of 4.5 mL/s, and CCTA image acquisition was performed using prospective ECG triggering. The acquisition and reconstruction parameters for the patients in our study were the following: 120 kV tube potential, tube current automatically adjusted according to patient body mass index (BMI), 275 ms/time gantry rotation speed, 0.5 mm slice increment, image reconstruction with a 512×512 matrix, and 0.25 or 0.5 mm increments. The collected data were transferred to a VitreaWorkstation fX (Vital Images, Minnetonka, MN, USA) for post-processing including multiplanar reformat (MPR), curved MPR, and volume reformat.

Quantification measurement of imaging indicators

According to our research requirements, the quantitative measurement of PCAT was performed semiautomatically using dedicated software (CoronarDoc version 1.11.1; Shukun Network Technology, Beijing, China). The software's PCAT analysis strictly followed the methodology previously defined by Oikonomou *et al.*, and PCAT was defined as the adipose tissue located within a radial distance from the outer vessel wall equal to the diameter of the coronary vessel and with the CT attenuation ranging from -190 to -30 Hounsfield units (HU) (7). The FAI was the average CT attenuation of PCAT (HU) (5,15). We respectively measured PCAT in the proximal 40-mm length range of the LAD and LCX, and in the 10- to 50-mm length segment proximal to the RCA. In addition to measuring the FAI within the radial distance from the outer vessel wall equal to the coronary vessel diameter, namely, the reference distance (FAI_{ref}), we also measured the FAI within a 2-mm radial distance closer to the outer vessel wall (FAI_{2mm}) and the FAI within a 6-mm radial distance further from the outer vessel wall (FAI_{6mm}) (Figure 2). For the measurement of PCAT around culprit and non-culprit lesions in patients with ACS, we performed lesion-specific FAI measurements centered on the most severe stenosis of the lesion, measured proximally and distally 5 mm from the center of the lesion, and all lesions measured 10 mm in length (Figure 3) (16). Furthermore, we measured the degree of coronary stenosis at each lesion in the included patients and calculated their Gensini score accordingly [detailed measurements in Supplementary file (Appendix 1)], which were used to assess the severity of CAD in the included patients (17). The above parameters were measured jointly by two experienced radiologists blinded to other test results.

Analysis of the FAI data

First, PCAT was analyzed at the vascular level. The Wilcoxon rank-sum test was used to compare the FAI around the culprit lesions with that of non-culprit lesions, and pairwise comparisons of the FAI within different radial distances from the outer vessel wall were also performed. Subsequently, correlation analysis was performed between the FAI of the 3 proximal coronary arteries within different radial distances from the outer wall of the vessel, and Pearson correlation analysis was performed between this FAI value and that of the culprit lesions.

Second, for patient stratification based on PCAT, we differentiated patients with UA from MI and respectively compared the FAI around culprit lesions and the FAI_{ref} proximal to the LAD in the two groups. In addition, patients with ACS and stable CAD were divided into a training set and an internal validation set at a ratio of 7:3. The parameters included in the logistic regression model were screened using univariate ($P < 0.10$) and multivariate logistic regression ($P < 0.05$). We then visualized the results of the multivariable logistic regression screening and plotted a forest plot and nomogram to express the relationships between variables in the model. The performance of the multivariable models was assessed with receiver operator characteristic (ROC) curves and decision curve analysis (DCA) curves. The ability of the FAI within different radial distances from the outer vessel wall in the proximal part of the 3 coronary arteries to identify patients with stable CAD and ACS was evaluated. Additionally, as this was a retrospective cross-sectional study, there were no missing data.

Statistical analysis

Statistical analysis was performed with R software (version 4.0.1; The R Foundation for Statistical Computing, Vienna, Austria). The normality of the continuous data was assessed using the Shapiro-Wilk test. Continuous variables are expressed as the mean \pm standard deviation (SD) of normally distributed variables, while nonnormally distributed variables are expressed as the median and interquartile range (IQR). Comparisons were made using Student *t*-test or Mann-Whitney test as needed. Categorical variables are expressed as absolute frequencies and percentages and were compared using the χ^2 test or Fisher exact test as appropriate. A 2-tailed *P* value < 0.05 was considered statistically significant.

Results

Clinical characteristics

A total of 267 patients were included in the study. The clinical characteristics of the enrolled ACS population are shown in Tables 1,2. The age of all patients with ACS was 63.84 ± 9.53 years, and 61.3% of the 173 patients were males. Among them, there were no significant differences between the included patients with MI and those with UA in terms of basic clinical information and risk factors (each *P* value

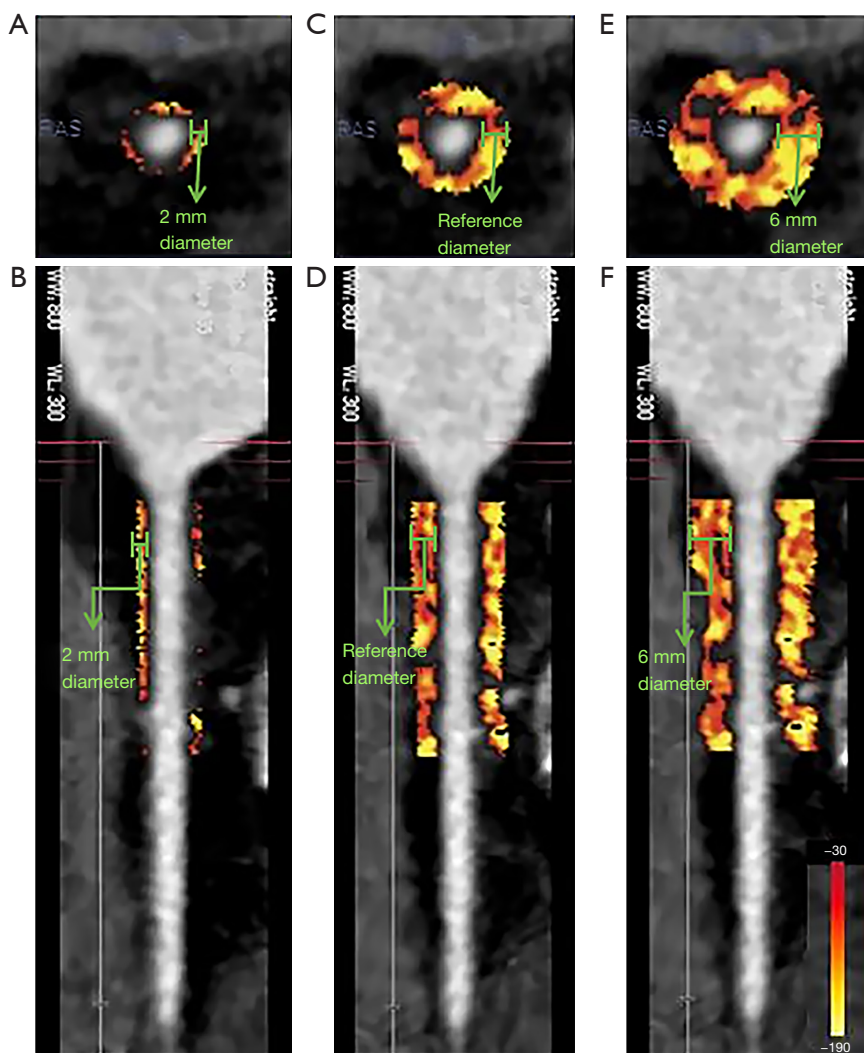


Figure 2 A case example of PCAT around the proximal RCA in a 66-year-old female patient with hypertension and diabetes mellitus. The PCAT is visualized with an adipose tissue HU color table shown with color bars. The following quantified PCATs around the proximal RCA from CTA are shown: pericoronary adipose tissue attenuation between -190 and -30 HU in the corresponding cross-sectional views (A,C,E) and straightened views (B,D,F), (A,B) the PCAT quantification around the proximal RCA (10–50 mm from the ostium) within a 2-mm diameter from the outer wall of the vessel, (C,D) the PCAT quantification around the proximal RCA (10–50 mm from the ostium) within the reference diameter from the outer wall of the vessel, and (E,F) the PCAT quantification around the proximal RCA (10–50 mm from the ostium) within a 6-mm diameter from the outer wall of the vessel. PCAT, pericoronary adipose tissue; RCA, right coronary artery; HU, Hounsfield unit.

>0.05). However, the FAI around culprit lesions in patients with MI was significantly higher than that in patients with UA (-73.15 ± 10.35 vs. -79.17 ± 10.13 ; $P=0.005$). Table 2 shows comparison between the training set and the test set, with no statistical difference in the variables between the two groups (each P value >0.05).

The FAI around the proximal coronary arteries

A total of 267 patients comprising 801 coronary vessels were included in the study, and 3 FAI parameters were measured per vessel, yielding a total of 2,403 parameters. The FAI_{2mm} of patients with ACS was significantly higher compared to FAI_{ref} and FAI_{6mm} in the proximal end of the

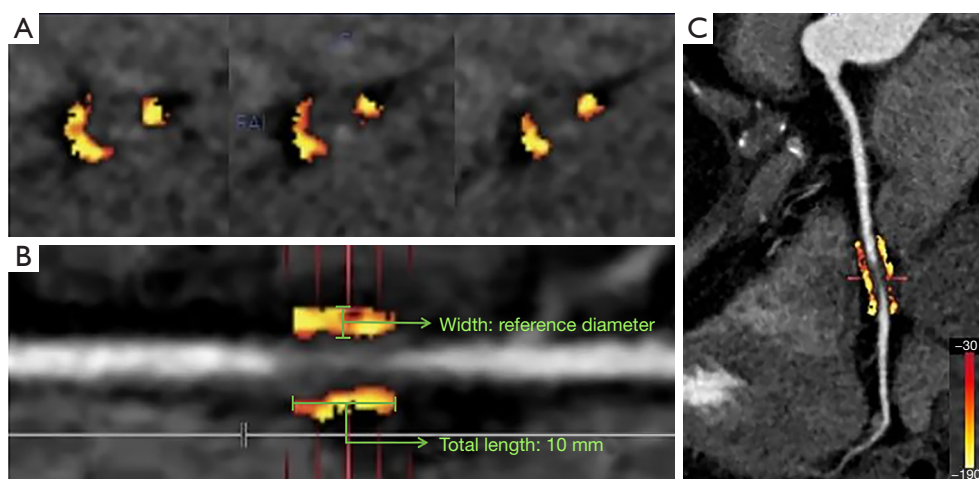


Figure 3 Semiautomatic measurement of the PCAT around the lesion on CCTA. PCAT is visualized with adipose tissue in the HU color table shown with color bars. The width of all lesions was measured as the reference diameter from the outer wall with a total length of 10 mm. (A) Corresponding cross-sectional views of the PCAT around the lesion are shown; (B) the segment of the lesion in a straightened view; (C) the curved multiplanar view showing the PCAT quantification of the lesion. PCAT, pericoronary adipose tissue; CCTA, computed tomography angiography.

RCA [$\text{FAI}_{2\text{mm}}$: -80.00 (-86.00 , -74.00); *vs.* FAI_{ref} : -86.00 (-92.00 , -81.00); $\text{FAI}_{6\text{mm}}$: -86.00 (-93.00 , -81.00); $P < 0.001$]; moreover, in the proximal end of the LAD and LCX, a significant improvement in the FAI was found when the radial expansion distance was 2 mm as compared to reference and 6 mm (each P value < 0.001 ; *Figure 4A*). As expected, similar changes were found in patients with stable CAD (each P value < 0.001 ; *Figure 4B*). *Figure 5A* shows the correlation between the FAI within different radial distances around coronary arteries in patients with ACS. There was a positive correlation between the FAI of any two segments measured (each P value < 0.001). Especially in the same coronary trunk, the correlation between the FAI within different radial distances was high (each P value < 0.001).

The FAI around culprit lesions

We included 202 (50.8%) culprit lesions and 196 (49.2%) non-culprit lesions. The FAI around culprit lesions was significantly different from that around non-culprit lesions [-78.00 (-84.00 , -72.00) *vs.* -90.00 (-97.50 , -83.00); $P < 0.001$; *Figure S1A*]. There were also significant differences in the FAI around culprits and non-culprit lesions on any coronary artery when subvessel comparisons were performed (each P value < 0.001 ; *Figure S1B*). The FAI

around culprit lesions was correlated with the FAI within different radial distances in the proximal coronary arteries (each P value < 0.001 ; *Figure 5A*). Among them, the FAI around culprit lesions was moderately to highly correlated with FAI_{ref} [$r = 0.540$; 95% confidence interval (CI): 0.434 – 0.631 ; $P < 0.001$] and $\text{FAI}_{6\text{mm}}$ ($r = 0.548$; 95% CI: 0.443 – 0.638 ; $P < 0.001$) proximal to the RCA, FAI_{ref} proximal to the LAD ($r = 0.587$; 95% CI: 0.489 – 0.671 ; $P < 0.001$), and the FAI_{ref} ($r = 0.586$; 95% CI: 0.487 – 0.670 ; $P < 0.001$) and $\text{FAI}_{6\text{mm}}$ ($r = 0.531$; 95% CI: 0.423 – 0.623 ; $P < 0.001$) proximal to the LCX (*Table S1*). Of these, the FAI surrounding culprit lesions was most associated with FAI_{ref} proximal to the LAD and LCX (*Figure 5B, 5C*). Additionally, we compared the correlation between different FAI and Gensini scores for all patients (*Table S2*) but did not find a significant correlation ($|r| < 0.3$).

Comparison of MI and UA

The FAI around culprit lesions was lower in patients with UA than in those with MI [-79.00 (-85.00 , -73.00) *vs.* -73.00 (-79.00 , -65.00); $P = 0.007$; *Figure S2A*], and FAI_{ref} proximal to the LAD was also lower in patients with UA than in those with MI [-84.00 (-90.00 , -78.00) *vs.* -81.00 (-85.00 , -73.50); $P = 0.02$] (*Figure S2B*).

Table 1 Comparison of clinical characteristics of patients with MI and UA

Variables	Patients with ACS (n=173)	MI (n=23)	UA (n=150)	P value
Patient characteristics				
Age (years)	63.84±9.53	64.61±10.12	63.72±9.47	0.68
Gender				0.79
Male	106 (61.3)	13 (56.5)	93 (62.0)	
Female	67 (38.7)	10 (43.5)	57 (38.0)	
BMI (kg/m ²)	24.90 (23.20, 27.30)	24.50 (23.20, 25.38)	25.20 (23.40, 27.40)	0.14
Risk factors				
Obesity	28 (16.2)	2 (8.7)	26 (17.3)	0.46
Smoking	60 (34.7)	10 (43.5)	50 (33.3)	0.47
Drinking	27 (15.6)	3 (13.0)	24 (16.0)	0.96
Hypertension				0.82
I	15 (8.7)	1 (4.3)	14 (9.3)	
II	25 (14.5)	4 (17.4)	21 (14.0)	
III	73 (42.2)	9 (39.1)	64 (42.7)	
Diabetes	56 (32.4)	9 (39.1)	47 (31.3)	0.61
Dyslipidemia	110 (63.6)	13 (56.5)	97 (64.7)	0.60
Family history	1 (0.6)	0 (0.0)	1 (0.7)	>0.99
Gensini score	40.00 (20.00, 58.50)	44.00 (32.25, 69.00)	40.00 (20.00, 58.00)	0.22
FAI around culprit lesions (HU)	-78.40±10.33	-73.15±10.35	-79.17±10.13	0.005
FAI around non-culprit lesions (HU)	-89.79±10.59	-86.14±11.91	-90.40±10.26	0.05
The number of culprit lesions	202 (50.8)	26 (48.1)	176 (51.2)	
The number of non-culprit lesions	196 (49.2)	28 (51.9)	168 (48.8)	

Values are mean ± standard deviation, median (interquartile range) or n (%). P values signify statistical significance and reflect the differences between the MI cohort and UA cohort. MI, myocardial infarction; UA, unstable angina; ACS, acute coronary syndrome; BMI, body mass index; FAI, fat attenuation index; HU, Hounsfield unit.

Recognition performance of the different models

In the univariable analysis (Table S3), we included age, hypertension, and dyslipidemia; Gensini score, the FAI around the proximal LAD within the reference diameter from the outer wall of the vessel (LAD_{ref}), and the FAI around the proximal LAD within a 6-mm diameter from the outer wall of the vessel (LAD_{6mm}) were also incorporated into the model (P<0.1). The forest plot (Figure S3) showed that age [odds ratio (OR): 1.04; 95% CI: 1.00–1.08; P=0.03] and Gensini score (OR: 1.03; 95% CI: 1.02–1.05; P<0.001) were independent predictors of ACS disease, and the risk of ACS increased with age and Gensini score. An example

of the probability of being identified as ACS for a given patient under the nomogram is shown in Figure 6, whereby the total score was determined based on the individual scores calculated using the nomogram. Analysis of the ROC curves showed that in the test set, the models that added the Gensini score [area under the curve (AUC): 0.615; 95% CI: 0.490–0.741] had improved efficacy in identifying patients with ACS as compared to the clinical model (AUC: 0.541; 95% CI: 0.406–0.676). The model with the addition of LAD_{ref} to the clinical and Gensini scores (AUC: 0.663; 95% CI: 0.540–0.785) and that with the addition of LAD_{6mm} (AUC: 0.654; 95% CI: 0.531–0.777) also better identified patients with ACS and stable CAD compared to

Table 2 Baseline characteristics of the training set and test set

Variables	Training set			Test set			P**
	Stable CAD (n=65)	ACS (n=121)	P*	Stable CAD (n=29)	ACS (n=52)	P*	
Patient characteristics							
Gender, n (%)			>0.99			>0.99	0.41
Male	38 (58.5)	72 (59.5)		19 (65.5)	34 (65.4)		
Female	27 (41.5)	49 (40.5)		10 (34.5)	18 (34.6)		
Age (years)	60.40±9.90	63.80±9.57	0.03	62.70±9.74	64.00±9.53	0.55	0.44
BMI (kg/m ²)	25.30 (23.10, 27.10)	25.10 (23.70, 27.30)	0.77	24.20 (22.30, 25.80)	24.80 (23.00, 27.00)	0.42	0.34
Risk factors							
Obesity, n (%)	10 (15.4)	22 (18.2)	0.78	4 (13.8)	6 (11.5)	0.74	0.41
Smoking, n (%)	21 (32.3)	45 (37.2)	0.62	13 (44.8)	15 (28.8)	0.23	>0.99
Drinking, n (%)	10 (15.4)	19 (15.7)	>0.99	2 (6.9)	8 (15.4)	0.32	0.62
Hypertension, n (%)			0.15			0.33	0.56
I	5 (7.7)	10 (8.3)		2 (6.9)	5 (9.6)		
II	9 (13.8)	18 (14.9)		9 (31.0)	7 (13.5)		
III	20 (30.8)	55 (45.5)		8 (27.6)	18 (34.6)		
Diabetes, n (%)	18 (27.7)	37 (30.6)	0.81	10 (34.5)	19 (36.5)	>0.99	0.39
Dyslipidemia, n (%)	34 (52.3)	79 (65.3)	0.12	18 (62.1)	31 (59.6)	>0.99	>0.99
Family history, n (%)	1 (1.5)	0 (0.0)	0.35	0 (0.0)	1 (1.92)	>0.99	0.52
Gensini score	24.00 (17.00, 46.00)	43.00 (23.00, 75.50)	0.07	21.00 (13.00, 33.00)	40.00 (20.00, 58.00)	<0.001	0.10
FAI around the proximal coronary (HU)							
RCA _{2mm}	-80.91±10.7	-80.18±10.3	0.66	-84.28±7.96	-79.62±9.07	0.02	0.50
RCA _{ref}	-87.95±10.80	-86.51±9.89	0.37	-90.28±8.48	-86.88±8.99	0.10	0.38
RCA _{6mm}	-88.25±10.40	-86.83±9.76	0.37	-91.21±8.71	-87.23±8.83	0.06	0.28
LAD _{2mm}	-80.32±9.86	-79.04±9.46	0.39	-80.79±9.02	-77.96±7.63	0.16	0.66
LAD _{ref}	-87.46±8.88	-84.62±9.44	0.04	-85.00 (-92.00, -81.00)	-83.00 (-87.25, -76.75)	0.05	0.36
LAD _{6mm}	-88.45±9.68	-86.03±8.72	0.10	-90.03±9.65	-85.44±7.16	0.03	0.86
LCX _{2mm}	-80.22±9.70	-79.97±9.27	0.87	-81.97±9.81	-78.67±8.13	0.13	0.87
LCX _{ref}	-84.85±9.18	-84.05±8.99	0.57	-86.38±8.62	-81.96±8.27	0.03	0.50
LCX _{6mm}	-87.95±9.05	-86.64±8.45	0.34	-89.59±9.33	-86.13±7.41	0.09	0.81

Values are mean ± standard deviation, median (interquartile range) or n (%). *P values reflect the differences between the patients with stable CAD and ACS. **P values reflect the differences between the training set and test set. CAD, coronary artery disease; ACS, acute coronary syndrome; BMI, body mass index; FAI, fat attenuation index; RCA_{2mm}, FAI around the proximal RCA within a 2-mm diameter from the outer vessel wall; RCA_{ref}, FAI around the proximal RCA within the reference diameter from the outer vessel wall; RCA_{6mm}, FAI around the proximal RCA within a 6-mm diameter from the outer vessel wall; LAD_{2mm}, FAI around the proximal LAD within a 2-mm diameter from the outer vessel wall; LAD_{ref}, FAI around the proximal LAD within the reference diameter from the outer vessel wall; LAD_{6mm}, FAI around the proximal LAD within a 6-mm diameter from the outer vessel wall; LCX_{2mm}, FAI around the proximal LCX within a 2-mm diameter from the outer vessel wall; LCX_{ref}, FAI around the proximal LCX within the reference diameter from the outer vessel wall; LCX_{6mm}, FAI around the proximal LCX within a 6-mm diameter from the outer vessel wall; RCA, right coronary artery; LCX, left circumflex artery.

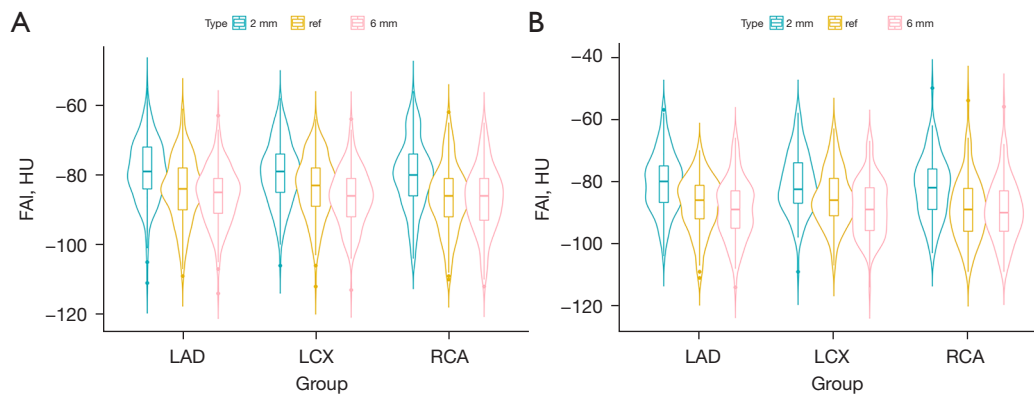


Figure 4 Comparison of the FAI of the 3 main coronary arteries within different radial distances in patients. (A) Comparison of the FAI in patients with ACS; (B) comparison of the FAI in patients with stable CAD. FAI, fat attenuation index; LAD, left anterior descending artery; LCX, left circumflex artery; RCA, right coronary artery; ACS, acute coronary syndrome; CAD, coronary artery disease.

the model with clinical features only (Figure 7A). However, it is clear that the model with the addition of LAD_{ref} had the highest discrimination efficacy among the models. Likewise, the DCA curve in the test indicated that the model based on clinical features, Gensini score, and LAD_{ref} produced greater gains set for identifying patients with ACS (Figure 7B).

Discussion

The key finding in this study was that culprit lesions were positively correlated with the FAI of either of the proximal coronary arteries, but the FAI_{ref} proximal to the LAD had the highest correlation with the FAI around culprit lesions, and it improved the identification performance for ACS and stable CAD. Therefore, LAD_{ref} can be used to monitor and identify inflammation in patients with ACS.

Adipose tissue can release bioactive substances that act on the blood vessel wall in an endocrine and paracrine manner (18). In the cardiovascular system, the activity of PCAT can secrete pro- and anti-inflammatory adipokines (19), causing vascular cells to secrete cytokines that maintain homeostasis. Various biological properties of PCAT are driven to a greater extent by the differentiation of preadipocytes into adipocytes, whereas the occurrence of inflammation can inhibit the differentiation of preadipocytes (20,21). Therefore, we can assume that coronary blood vessels and PCAT have a bidirectional role and that both are affected by each other's status. The CANTOS (Canakinumab Anti-Inflammatory Thrombosis Outcome Study) trial confirmed that vascular inflammation

inhibits local lipogenesis of PCAT (22), making it possible to noninvasively detect vascular inflammation using CCTA. Furthermore, the FAI overcomes many limitations of ^{18}F -fluorodeoxyglucose (^{18}F -FDG)-PET/CT to quantify inflammation, such as high cost, high radiation, and low availability (23,24). Additionally, the FAI can capture the dynamic inflammatory load of coronary vessels, which can be used to track longitudinal changes in coronary inflammation (25). Furthermore, the FAI has been found to be more sensitive and specific for the detection of coronary vascular inflammation as compared to systemic inflammatory biomarkers obtained from laboratory tests, such as hematology (26). Therefore, the FAI has been used as a routine, noninvasive quantitative index in the studies on coronary inflammation in recent years. ACS is caused by pathological etiologies such as rupture, erosion, or calcified nodules. However, recent studies have suggested that ACS primarily arises due to plaque rupture rather than plaque erosion (26). We speculated that this may be because plaque rupture involves higher inflammatory changes and vulnerable plaque features, such as greater macrophage infiltration and lipid burden (27) and that the inflammatory cell types differ between plaque erosion and plaque rupture, which also results in a higher degree of inflammation (28).

Although previous research has examined the possible correlation between epicardial adipose tissue (EAT) and the development of cardiovascular disease (29), we sought to evaluate PCAT. This is mainly because, although EAT can be measured to a greater extent and is more closely related to the myocardium, PCAT is in direct contact with the vasculature, can more directly receive the effect

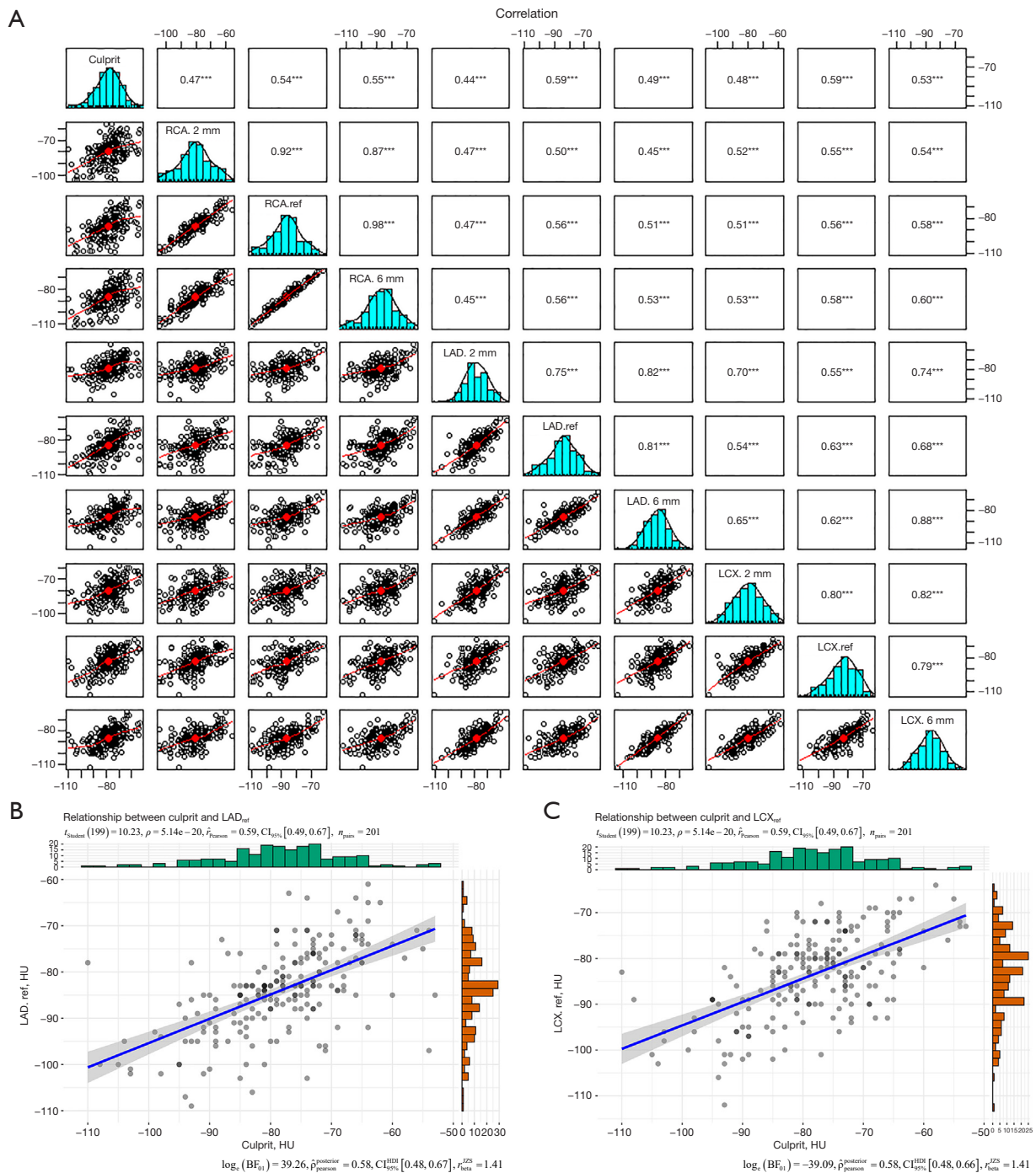


Figure 5 Pairwise correlations between FAIs based on different sites around coronary vessels. (A) Correlation between FAIs within different radial distances around the coronary artery. The diagonal line represents the normal distribution histogram of the data of different coronary proximal FAIs. The top of the diagonal line is the correlation r value and the significance level (indicated by asterisks) for the pairwise comparison of different FAIs, where *** represents $P < 0.001$, and the bottom of the diagonal is shown as a binary scatterplot with fitted lines. (B) Correlation between the FAI around culprit lesions and LAD_{ref}. (C) Correlation between the FAI around culprit lesions and LCX_{ref}. FAI, fat attenuation index; LAD, left anterior descending artery; LCX, left circumflex artery; LAD_{ref}, FAI around the proximal LAD within the reference diameter from the outer vessel wall; LCX_{ref}, FAI around the proximal LCX within the reference diameter from the outer vessel wall.

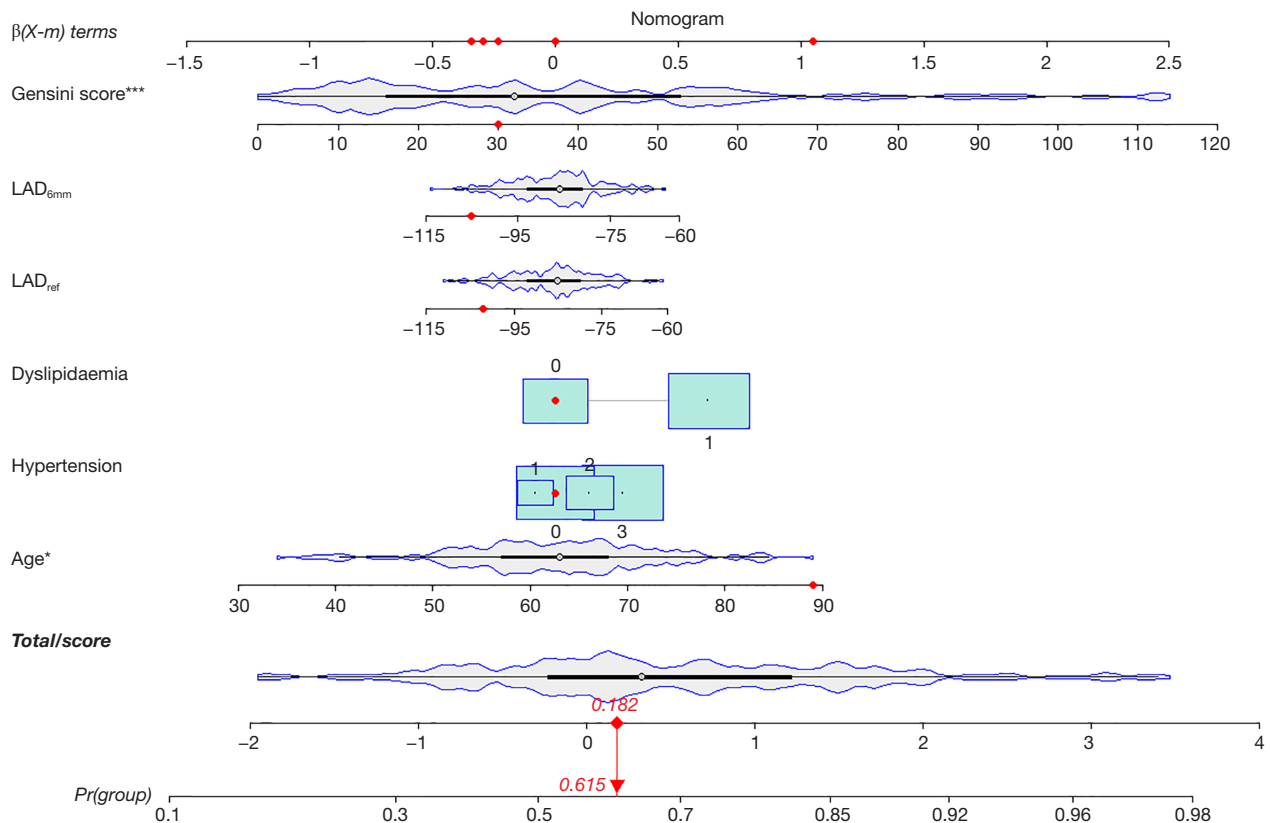


Figure 6 Example of a nomogram model prediction for ACS. Density plot of total score, age, Gensini score, LAD_{ref} , and LAD_{6mm} shows their distribution. For categorical variables, the distributions are reflected by the size of the box. Each point that corresponds to each variable is on the uppermost β terms. The sum of all points is the total score. The patient was 89 years old, did not have dyslipidemia or hypertension, and the LAD_{ref} and LAD_{6mm} were -102 and -105 HU, respectively, in addition with a Gensini score of 30. The point total projected at the bottom scale indicates the probability (61.5%) of the patient being identified with ACS. *, $P < 0.05$; ***, $P < 0.001$. LAD, left anterior descending artery; LAD_{6mm} , FAI around the proximal LAD within a 6-mm diameter from the outer wall of the vessel; LAD_{ref} , FAI around the proximal LAD within the reference diameter from the outer vessel wall; ACS, acute coronary syndrome; HU, Hounsfield units; FAI, fat attenuation index.

of the vasculature on the signaling factors secreted by the surrounding adipose tissue, responds more sensitively to inflammatory changes in the vasculature (30), and is thus more accurate than EAT (7). In previous research, PCAT proximal to the RCA was selected as a representative marker of coronary inflammation for the analysis of PCAT in each participant (7). For FAI measurements around the lesion sites, we referred to previous studies, but there may be limitations to this method for some diffuse or focal lesions. For diffuse lesions, it may not be possible to cover all areas, but the central location of the most severe lesion is included, whereas for focal lesions, normal adipose tissue may be included, but CAD is considered to undergo global inflammatory changes, with inflammatory changes

occurring in adipose tissue outside the lesion sites. Most of the similar studies measured PCAT at the maximum coronary stenosis (16,31), mainly because the culprit lesions are usually implanted with coronary stents, and the metal artifacts may affect the measurement of PCAT. In contrast, we obtained CCTA images of the enrolled patients before ICA and found a positive correlation between PCAT within different radial distances from the vessel wall proximal to the three major coronary arteries. Through the comparison, we inferred that the effect of vascular inflammation on PCAT is related to its distance from the vessel wall. FAI_{6mm} was not statistically significantly different compared to FAI_{ref} , although it was reduced; we speculate that the reduction in the FAI might not have been significant due

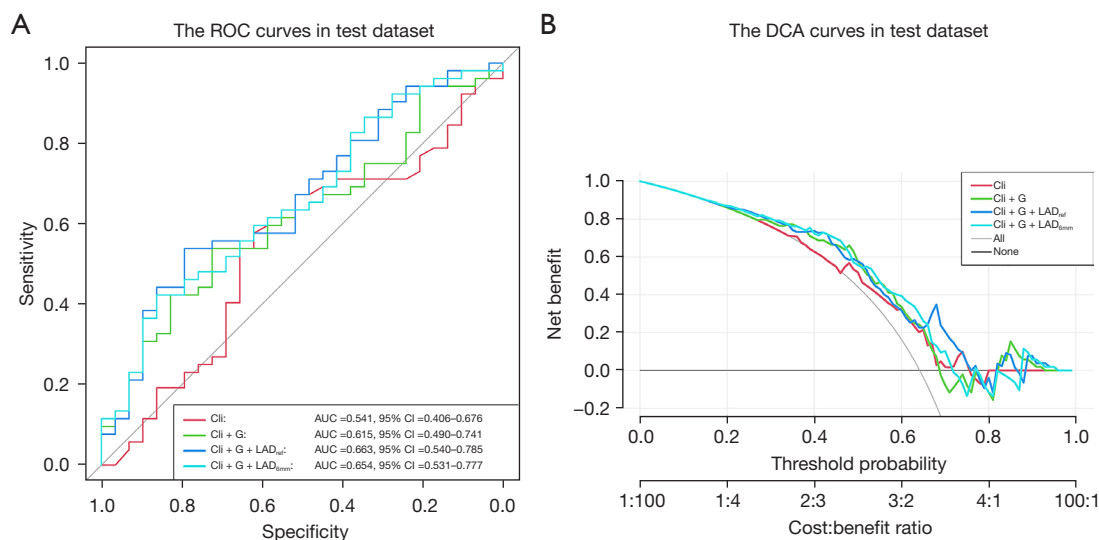


Figure 7 The prediction models for identifying patients with ACS. (A) ROC curves of the different models for identifying patients with ACS; (B) DCA for evaluating the 4 models for identifying patients with ACS. ROC, receiver operator characteristic; Cli, clinical features; G, Gensini score; LAD_{ref}, FAI around the proximal LAD within reference diameter from the outer vessel wall; LAD_{6mm}, FAI around the proximal LAD within a 6-mm diameter from the outer vessel wall; AUC, area under the curve; CI, confidence interval; DCA, decision curve analysis; ACS, acute coronary syndrome; FAI, fat attenuation index.

to the inclusion of some nonadipose tissue as the distance increased. However, we still included FAI_{6mm} in the study because there is molecular biology research showing that in patients with CAD, the FAI obtained by measuring in 1-mm increments from the layer immediately adjacent to the coronary vessel wall to a distance of 20 mm from the vessel wall gradually decreases to more negative values with increasing distance (5). Additionally, we found a positive correlation between the FAI around culprit lesions and the FAI within any radial distance proximal to the coronary arteries; moreover, the FAI_{ref} proximal to the LAD and LCX had the highest correlation with the FAI around culprit lesions. However, due to the small caliber and high probability of variation in anatomical structures of the LCX (25), we excluded it and concluded that the FAI_{ref} proximal to the LAD could best represent the inflammation of the culprit lesions in patients with ACS. Past studies have shown that patients with CAD have histological evidence of local inflammation (32), and the diffuse inflammation in PCAT is independent of the lesion site (33). Our findings further demonstrate that the changes of PCAT in patients with ACS are not affected by the location of culprit lesions, which is a global inflammation; that is, PCAT in proximal coronary arteries may produce diffuse inflammatory manifestations due to inflammatory changes in any part of

the coronary tree.

One study suggested that an increase in the FAI around the proximal RCA and LAD on CCTA images may be associated with an increased risk of cardiac death (7). We found that patients with MI had a higher FAI around culprit lesions than did the patients with UA, as both MI and UA are caused by myocardial damage, whereas patients with MI have myocardial necrosis and a more severe inflammatory state (34). We also found that the FAI in other components, including non-culprit lesions and LAD_{ref} to be higher in patients with MI than in those with UA; this is because patients with ACS are thought to have globally active coronary inflammation (34); that is, both patients with MI and UA develop diffuse inflammation due to a particular lesion, and as illustrated above, overall inflammation is more severe in patients with MI than in those with UA, thus causing the FAI around non-culprit lesions to be also higher in MI than in UA. Lin *et al.* (6) found that the FAI proximal to the RCA could distinguish patients with stable CAD from those with acute MI, thus indicating that PCAT attenuation could be used as an indicator of CAD stratification. In contrast to findings from basic biology research (5), Ueno *et al.* (13) found that the proximal FAI_{2mm} of the RCA had a higher diagnostic performance for predicting VSA than did the reference diameter of the

FAI. Therefore, we measured the FAI of the proximal end of the three main coronary arteries within the radial distance from the outer vessel wall of 2 mm, reference distance, and 6 mm on the basis of previous studies, and differentiated between patients with stable CAD and ACS by establishing ROC curves. It was found that the inclusion of LAD_{ref} based on the model that included clinical features and Gensini scores further improved the identification of patients with ACS. LAD_{6mm} was less effective compared to LAD_{ref} , which we believe may be due to the inclusion of non-fatty structures, such as the myocardium and coronary veins; in addition, closer adipose tissue may be affected by vascular pulsation. We speculate that reason for the RCA being excluded and the LAD being included was that atherosclerosis occurs more often in the LAD in clinical practice (35).

In view of the above findings, this study has the following implications. In patients with CAD, overall cardiac inflammation can be monitored by measuring the FAI_{ref} proximal to the LAD after conventional CCTA; patients with ACS with a higher burden of coronary inflammation can be initially identified before interventional examination; meanwhile, for less-severe situations, such as in patients with stable CAD, the over examination and overtreatment with intervention can be avoided, and the physical burden can be reduced. Moreover, quantitative measurement of the FAI after CCTA does not require patients to receive additional radiation doses or incur further costs. Moreover, the FAI_{ref} of the LAD can be automatically measured on software, which greatly improves the repeatability of the operation. In addition, research has shown that the FAI is not a static value and can change with treatment (36). Therefore, we can also infer the progression and prognosis of culprit lesions by observing the changes of the FAI_{ref} proximal to the LAD. We aim to conduct a follow-up study along this direction. In other future studies on coronary inflammation in patients with ACS, the FAI_{ref} proximal to the LAD can be measured more accurately and conveniently to quantify cardiac inflammatory changes, improving upon past methodologies for measuring PCAT around the RCA.

This study also has certain limitations. First, it employed a retrospective observational design using data from a single center with a relatively small number of patients, with all patients undergoing the same CT scanner and protocol, and thus there may be selection bias. Second, our study demonstrated there to be an association between the PCAT surrounding culprit lesions and the PCAT proximal to the coronary arteries, but we did not assume a direct

causal relationship between the two values. Third, the information on patients' medication was not included in our clinical characteristics mainly because some patients did not take their medication regularly or were unable to keep detailed records of the medication used. Finally, the spatial resolution of CT may limit PCAT assessment in small amounts of adipose tissue and adjacent severe coronary artery calcification, which might have produced partial volume averaging effects.

Conclusions

In patients with ACS, the FAI_{ref} around the proximal LAD demonstrated the highest correlation with the FAI around culprit lesions, which could be used to represent whole heart inflammation and could improve the identification of patients with ACS and stable CAD before intervention.

Acknowledgments

Funding: This work was supported by the Beijing Cihua Medical Development Foundation Project (research on CT-assisted diagnosis of coronary heart disease based on artificial intelligence); the Fourth Affiliated Hospital of Harbin Medical University (molecular imaging of myocardial oxidative stress response in obese states: No. HYDSYTB202228); and the Fourth Affiliated Hospital of Harbin Medical University (PD-L1 inhibitors in combination with targeted agents for kidney cancer treatment and molecular imaging: No. JD22C007).

Footnote

Reporting Checklist: The authors have completed the STROBE reporting checklist. Available at <https://qims.amegroups.com/article/view/10.21037/qims-22-864/rc>

Conflicts of Interest: All authors have completed the ICMJE uniform disclosure form (available at <https://qims.amegroups.com/article/view/10.21037/qims-22-864/coif>). MZ is a current employee of GE Healthcare. The other authors have no conflicts of interest to declare.

Ethical Statement: The authors are accountable for all aspects of the work in ensuring that questions related to the accuracy or integrity of any part of the work are appropriately investigated and resolved. The study was conducted in accordance with the Declaration of Helsinki (as

revised in 2013). The study was approved by the Medical Ethics Committee of the Fourth Affiliated Hospital of Harbin Medical University (No. 2022-SCILLSC-13), and individual consent for this retrospective analysis was waived.

Open Access Statement: This is an Open Access article distributed in accordance with the Creative Commons Attribution-NonCommercial-NoDerivs 4.0 International License (CC BY-NC-ND 4.0), which permits the non-commercial replication and distribution of the article with the strict proviso that no changes or edits are made and the original work is properly cited (including links to both the formal publication through the relevant DOI and the license). See: <https://creativecommons.org/licenses/by-nc-nd/4.0/>.

References

- Shi K, Yang FF, Si N, Zhu CT, Li N, Dong XL, Guo Y, Zhang T. Effect of 320-row CT reconstruction technology on fractional flow reserve derived from coronary CT angiography based on machine learning: single- versus multiple-cardiac periodic images. *Quant Imaging Med Surg* 2022;12:3092-103.
- Santos-Gallego CG, Picatoste B, Badimón JJ. Pathophysiology of acute coronary syndrome. *Curr Atheroscler Rep* 2014;16:401.
- Libby P. Inflammation in atherosclerosis. *Arterioscler Thromb Vasc Biol* 2012;32:2045-51.
- Libby P, Tabas I, Fredman G, Fisher EA. Inflammation and its resolution as determinants of acute coronary syndromes. *Circ Res* 2014;114:1867-79.
- Antonopoulos AS, Sanna F, Sabharwal N, Thomas S, Oikonomou EK, Herdman L, et al. Detecting human coronary inflammation by imaging perivascular fat. *Sci Transl Med* 2017;9:eal2658.
- Lin A, Nerlekar N, Yuvaraj J, Fernandes K, Jiang C, Nicholls SJ, Dey D, Wong DTL. Pericoronary adipose tissue computed tomography attenuation distinguishes different stages of coronary artery disease: a cross-sectional study. *Eur Heart J Cardiovasc Imaging* 2021;22:298-306.
- Oikonomou EK, Marwan M, Desai MY, Mancio J, Alashi A, Hutt Centeno E, et al. Non-invasive detection of coronary inflammation using computed tomography and prediction of residual cardiovascular risk (the CRISP CT study): a post-hoc analysis of prospective outcome data. *Lancet* 2018;392:929-39.
- Stefanadis C, Toutouzas K, Tsiamis E, Stratos C, Vavuranakis M, Kallikazaros I, Panagiotakos D, Toutouzas P. Increased local temperature in human coronary atherosclerotic plaques: an independent predictor of clinical outcome in patients undergoing a percutaneous coronary intervention. *J Am Coll Cardiol* 2001;37:1277-83.
- Joshi NV, Vesey AT, Williams MC, Shah AS, Calvert PA, Craighead FH, Yeoh SE, Wallace W, Salter D, Fletcher AM, van Beek EJ, Flapan AD, Uren NG, Behan MW, Cruden NL, Mills NL, Fox KA, Rudd JH, Dweck MR, Newby DE. 18F-fluoride positron emission tomography for identification of ruptured and high-risk coronary atherosclerotic plaques: a prospective clinical trial. *Lancet* 2014;383:705-13.
- Camici PG, Rimoldi OE, Gaemperli O, Libby P. Non-invasive anatomic and functional imaging of vascular inflammation and unstable plaque. *Eur Heart J* 2012;33:1309-17.
- Fleg JL, Stone GW, Fayad ZA, Granada JF, Hatsukami TS, Kolodgie FD, Ohayon J, Pettigrew R, Sabatine MS, Tearney GJ, Waxman S, Domanski MJ, Srinivas PR, Narula J. Detection of high-risk atherosclerotic plaque: report of the NHLBI Working Group on current status and future directions. *JACC Cardiovasc Imaging* 2012;5:941-55.
- Sugiyama T, Kanaji Y, Hoshino M, Yamaguchi M, Hada M, Ohya H, Sumino Y, Hirano H, Kanno Y, Horie T, Misawa T, Nogami K, Ueno H, Hamaya R, Usui E, Murai T, Lee T, Yonetsu T, Sasano T, Kakuta T. Determinants of Pericoronary Adipose Tissue Attenuation on Computed Tomography Angiography in Coronary Artery Disease. *J Am Heart Assoc* 2020;9:e016202.
- Ueno H, Hoshino M, Sugiyama T, Kanaji Y, Nogami K, Horie T, Yamaguchi M, Hada M, Sumino Y, Misawa T, Hirano H, Yonetsu T, Sasano T, Kakuta T. Pericoronary Adipose Tissue Inflammation on Coronary Computed Tomography in Patients With Vasospastic Angina. *JACC Cardiovasc Imaging* 2021;14:511-2.
- Collet JP, Thiele H, Barbato E, Barthélémy O, Bauersachs J, Bhatt DL, et al. 2020 ESC Guidelines for the management of acute coronary syndromes in patients presenting without persistent ST-segment elevation. *Eur Heart J* 2021;42:1289-367. Erratum in: *Eur Heart J* 2021;42:1908. Erratum in: *Eur Heart J* 2021;42:1925. Erratum in: *Eur Heart J* 2021. PMID: 32860058.
- Goeller M, Tamarappoo BK, Kwan AC, Cadet S,

- Commandeur F, Razipour A, Slomka PJ, Gransar H, Chen X, Otaki Y, Friedman JD, Cao JJ, Albrecht MH, Bittner DO, Marwan M, Achenbach S, Berman DS, Dey D. Relationship between changes in pericoronary adipose tissue attenuation and coronary plaque burden quantified from coronary computed tomography angiography. *Eur Heart J Cardiovasc Imaging* 2019;20:636-43.
16. Ma R, van Assen M, Ties D, Pelgrim GJ, van Dijk R, Sidorenkov G, van Ooijen PMA, van der Harst P, Vliegenthart R. Focal pericoronary adipose tissue attenuation is related to plaque presence, plaque type, and stenosis severity in coronary CTA. *Eur Radiol* 2021;31:7251-61.
 17. Gao X, Mi S, Zhang F, Gong F, Lai Y, Gao F, Zhang X, Wang L, Tao H. Association of chemerin mRNA expression in human epicardial adipose tissue with coronary atherosclerosis. *Cardiovasc Diabetol* 2011;10:87.
 18. Antoniadou C, Antonopoulos AS, Tousoulis D, Stefanadis C. Adiponectin: from obesity to cardiovascular disease. *Obes Rev* 2009;10:269-79.
 19. Pou KM, Massaro JM, Hoffmann U, Vasan RS, Maurovich-Horvat P, Larson MG, Keaney JF Jr, Meigs JB, Lipinska I, Kathiresan S, Murabito JM, O'Donnell CJ, Benjamin EJ, Fox CS. Visceral and subcutaneous adipose tissue volumes are cross-sectionally related to markers of inflammation and oxidative stress: the Framingham Heart Study. *Circulation* 2007;116:1234-41.
 20. Grant RW, Stephens JM. Fat in flames: influence of cytokines and pattern recognition receptors on adipocyte lipolysis. *Am J Physiol Endocrinol Metab* 2015;309:E205-13.
 21. Ntambi JM, Young-Cheul K. Adipocyte differentiation and gene expression. *J Nutr* 2000;130:3122S-6S.
 22. Ridker PM, Everett BM, Thuren T, MacFadyen JG, Chang WH, Ballantyne C, et al. Antiinflammatory Therapy with Canakinumab for Atherosclerotic Disease. *N Engl J Med* 2017;377:1119-31.
 23. Antonopoulos AS, Antoniadou C. Perivascular Fat Attenuation Index by Computed Tomography as a Metric of Coronary Inflammation. *J Am Coll Cardiol* 2018;71:2708-9.
 24. Mancio J, Oikonomou EK, Antoniadou C. Perivascular adipose tissue and coronary atherosclerosis. *Heart* 2018;104:1654-62.
 25. Oikonomou EK, Williams MC, Kotanidis CP, Desai MY, Marwan M, Antonopoulos AS, et al. A novel machine learning-derived radiotranscriptomic signature of perivascular fat improves cardiac risk prediction using coronary CT angiography. *Eur Heart J* 2019;40:3529-43.
 26. Nakajima A, Sugiyama T, Araki M, Seegers LM, Dey D, McNulty I, Lee H, Yonetsu T, Yasui Y, Teng Y, Nagamine T, Nakamura S, Achenbach S, Kakuta T, Jang IK. Plaque Rupture, Compared With Plaque Erosion, Is Associated With a Higher Level of Pancoronary Inflammation. *JACC Cardiovasc Imaging* 2022;15:828-39.
 27. Yamamoto E, Yonetsu T, Kakuta T, Soeda T, Saito Y, Yan BP, et al. Clinical and Laboratory Predictors for Plaque Erosion in Patients With Acute Coronary Syndromes. *J Am Heart Assoc* 2019;8:e012322.
 28. Leistner DM, Kränkel N, Meteva D, Abdelwahed YS, Seppelt C, Stähli BE, et al. Differential immunological signature at the culprit site distinguishes acute coronary syndrome with intact from acute coronary syndrome with ruptured fibrous cap: results from the prospective translational OPTICO-ACS study. *Eur Heart J* 2020;41:3549-60.
 29. Christensen RH, von Scholten BJ, Lehrskov LL, Rossing P, Jørgensen PG. Epicardial adipose tissue: an emerging biomarker of cardiovascular complications in type 2 diabetes? *Ther Adv Endocrinol Metab* 2020;11:2042018820928824.
 30. Oikonomou EK, Antoniadou C. The role of adipose tissue in cardiovascular health and disease. *Nat Rev Cardiol* 2019;16:83-99.
 31. Lin A, Kolossváry M, Yuvaraj J, Cadet S, McElhinney PA, Jiang C, Nerlekar N, Nicholls SJ, Slomka PJ, Maurovich-Horvat P, Wong DTL, Dey D. Myocardial Infarction Associates With a Distinct Pericoronary Adipose Tissue Radiomic Phenotype: A Prospective Case-Control Study. *JACC Cardiovasc Imaging* 2020;13:2371-83.
 32. Bentzon JF, Otsuka F, Virmani R, Falk E. Mechanisms of plaque formation and rupture. *Circ Res* 2014;114:1852-66.
 33. Sugiyama T, Yamamoto E, Bryniarski K, Xing L, Lee H, Isobe M, Libby P, Jang IK. Nonculprit Plaque Characteristics in Patients With Acute Coronary Syndrome Caused by Plaque Erosion vs Plaque Rupture: A 3-Vessel Optical Coherence Tomography Study. *JAMA Cardiol* 2018;3:207-14.
 34. Si N, Shi K, Li N, Dong X, Zhu C, Guo Y, Hu J, Cui J, Yang F, Zhang T. Identification of patients with acute myocardial infarction based on coronary CT angiography: the value of pericoronary adipose tissue radiomics. *Eur Radiol* 2022;32:6868-77.
 35. Bhatia HS, Lin F, Thomas IC, Denenberg J, Kandula NR, Budoff MJ, Criqui MH, Kanaya AM. Coronary artery calcium incidence and changes using direct plaque

measurements: The MASALA study. *Atherosclerosis* 2022;353:41-6.
36. Dai X, Yu L, Lu Z, Shen C, Tao X, Zhang J. Serial change

of perivascular fat attenuation index after statin treatment: Insights from a coronary CT angiography follow-up study. *Int J Cardiol* 2020;319:144-9.

Cite this article as: Dong X, Zhu C, Li N, Shi K, Si N, Wang Y, Pan H, Shi Z, Wang S, Zhao M, Zhang T. Identification of patients with acute coronary syndrome and representation of their degree of inflammation: application of pericoronary adipose tissue within different radial distances of the proximal coronary arteries. *Quant Imaging Med Surg* 2023;13(6):3644-3659. doi: 10.21037/qims-22-864

Appendix 1

Methods

Participants and study design

Specific identification of the culprit lesions

At least 2 of the following morphological features suggestive of acute plaque rupture should be present:

- (A) Intraluminal filling defects consistent with thrombus (i.e., acute occlusion abruptly ending with a squared-off or convex upstream termination, or an intraluminal filling defect in a patent vessel within or adjacent to a stenotic region with surrounding homogeneous contrast opacification);
- (B) Plaque ulceration (i.e., presence of contrast and hazy contour beyond the vessel lumen);
- (C) Plaque irregularity (i.e., irregular margins or overhanging edges), dissection, or impaired flow.

Definition of cardiovascular risk factors

Baseline patient characteristics were collected from inpatient medical records. Clinical data on age, gender, body mass index (BMI), and cardiovascular risk factors were analyzed. The classification criteria for cardiovascular risk factors were as follows:

- (A) hypertension, defined as systolic blood pressure >140 mmHg and/or diastolic blood pressure >90 mmHg and/or use of antihypertensive drugs according to guidelines (37);
- (B) dyslipidemia, defined as a fasting total cholesterol >6.2 mmol/L, low-density lipoprotein cholesterol (LDL-C) >3.4 mmol/L, high-density lipoprotein cholesterol <1.0 mmol/L, serum triglycerides >1.7 mmol/L (outpatients only), or diagnosis/treatment of dyslipidemia (38);
- (C) diabetes mellitus, defined as a fasting blood glucose level ≥ 7.0 mmol/L or glycosylated hemoglobin (HbA1c) level $\geq 6.5\%$ (39);
- (D) smoker, defined as current active or former smokers; and
- (E) family history of coronary artery disease, defined as a family history of ≥ 1 degree of consanguinity with coronary artery disease before the age of 60 (6);
- (F) additionally, patients with a BMI ≥ 28 kg/m² were considered obese.

Quantification measurement of imaging indicators

The Gensini score method (40) was used to assess the degree of coronary stenosis, with the most severe stenosis used as the site of stenosis for scoring. A stenosis diameter of $<25\%$ was scored as 1 point, 25–49% as 2 points, 50–74% as 4 points, 75–89% as 8 points, 90–99% as 16 points, and total occlusion as 32 points. The above scores were multiplied by a corresponding coefficient: 5 for the left main branch (LM); 2.5 and 1.5 for the proximal and middle segment of the LAD, respectively; 1 and 0.5 for the D1 and D2 in the diagonal branches, respectively; 2.5 and 1 for the proximal and distal segment lesions of the LCX, respectively; and 1 for the proximal, middle, distal, and posterior descending branch lesions of the RCA. The sum of the scores for each lesion is the patient's coronary stenosis total score.

Results

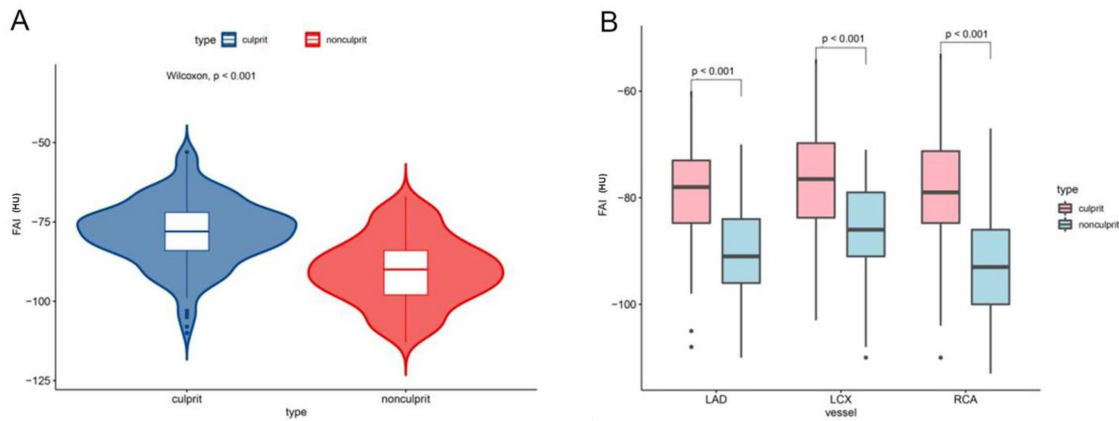


Figure S1 Comparison of FAI around culprit lesions and non-culprit lesions in patients with ACS. (A) Comparison of differences between all culprit lesions and non-culprit lesions in the group. (B) Comparison of the culprit and non-culprit lesions located within the same vessel across all vessels enrolled. FAI, fat attenuation index; ACS, acute coronary syndrome; LAD, left anterior descending artery; RCA, right coronary artery; LCX, left circumflex artery.

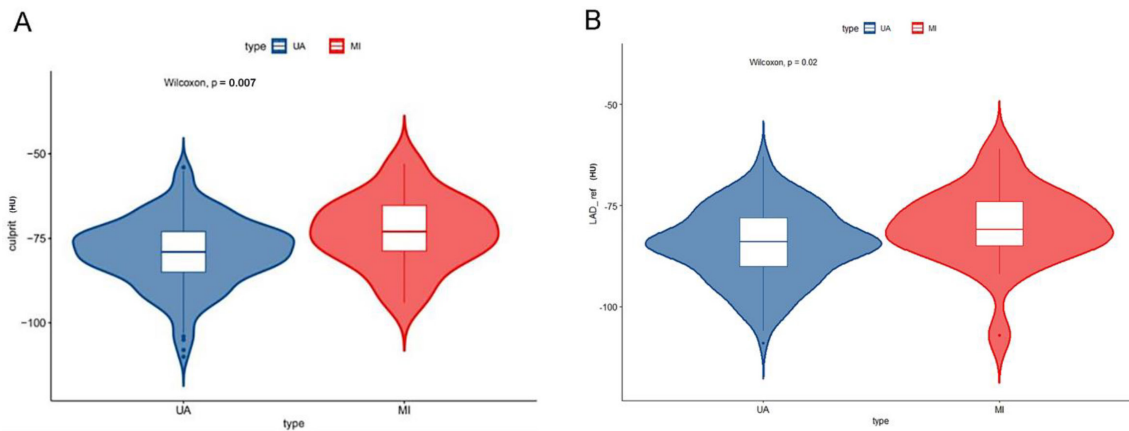


Figure S2 Comparison of FAI in patients with UA and MI. (A) Comparison of FAI around culprit lesions in patients with UA and MI. (B) Comparison of LAD_ref in patients with UA and MI. FAI, fat attenuation index; UA, unstable angina; MI, myocardial infarction; FAI, fat attenuation index; LAD_ref, FAI around the proximal LAD within reference diameter from the outer vessel wall.

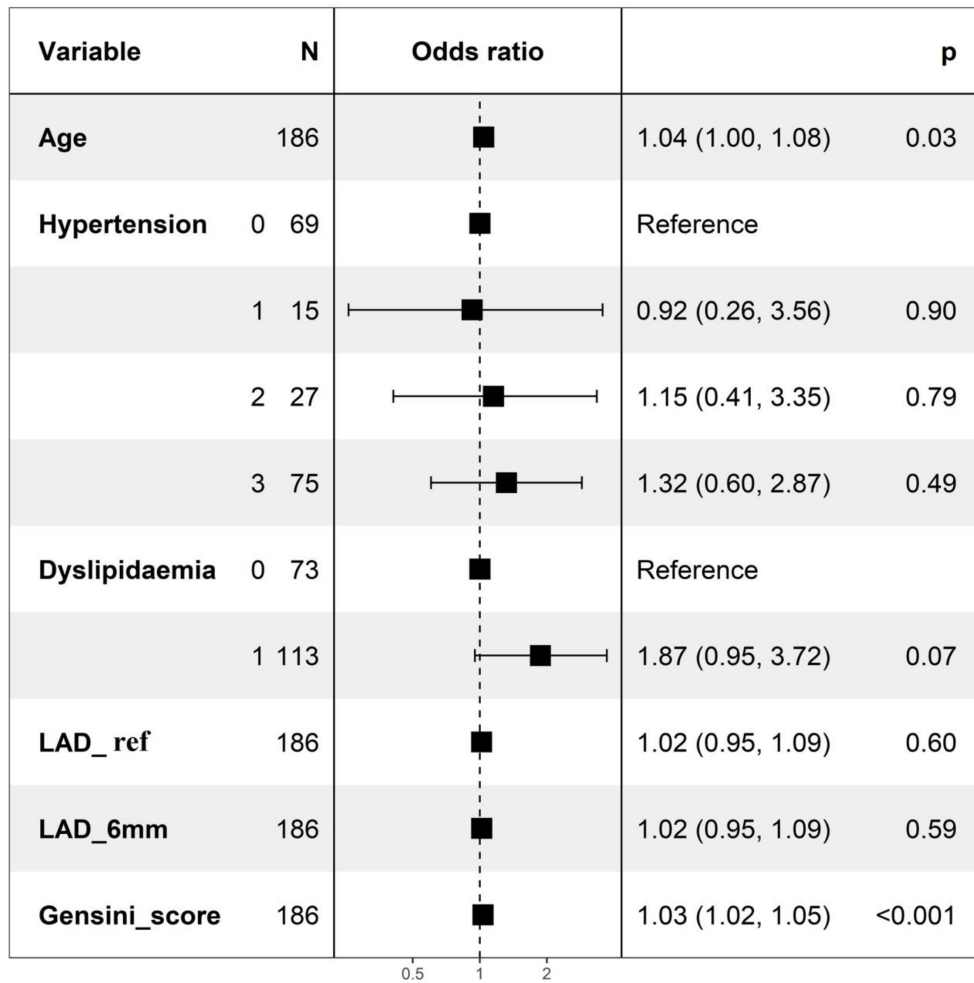


Figure S3 Forest plot of the model for identifying patients with ACS. ACS, acute coronary syndrome; LAD, left anterior descending artery; FAI, fat attenuation index; LAD_ref, FAI around the proximal LAD within reference diameter from the outer vessel wall; LAD_6mm, FAI around the proximal LAD within a 6-mm diameter from the outer vessel wall.

Table S1 Correlation of the FAI around culprit lesions with the FAI around different radial distances proximal to the coronary artery in patients with ACS

	r (95% CI)	P
RCA_2mm	0.473 (0.358–0.574)	<0.001
RCA_ref	0.540 (0.434–0.631)	<0.001
RCA_6mm	0.548 (0.443–0.638)	<0.001
LAD_2mm	0.438 (0.319–0.543)	<0.001
LAD_ref	0.587 (0.489–0.671)	<0.001
LAD_6mm	0.490 (0.377–0.589)	<0.001
LCX_2mm	0.484 (0.370–0.583)	<0.001
LCX_ref	0.586 (0.487–0.670)	<0.001
LCX_6mm	0.531 (0.423–0.623)	<0.001

FAI, fat attenuation index; ACS, acute coronary syndrome; RCA, right coronary artery; LAD, left anterior descending artery; LCX, left circumflex artery; RCA_2mm, FAI around the proximal RCA within a 2-mm diameter from the outer vessel wall; RCA_ref, FAI around the proximal RCA within reference diameter from the outer vessel wall; RCA_6mm, FAI around the proximal RCA within a 6-mm diameter from the outer vessel wall; LAD_2mm, FAI around the proximal LAD within a 2-mm diameter from the outer vessel wall; LAD_ref, FAI around the proximal LAD within reference diameter from the outer vessel wall; LAD_6mm, FAI around the proximal LAD within a 6-mm diameter from the outer vessel wall; LCX_2mm, FAI around the proximal LCX within a 2-mm diameter from the outer vessel wall; LCX_ref, FAI around the proximal LCX within reference diameter from the outer vessel wall; LCX_6mm, FAI around the proximal LCX within a 6-mm diameter from the outer vessel wall.

Table S2 Correlation of Gensini score with the FAI around different radial distances proximal to the coronary artery in all patients

	r (95% CI)	P
RCA_2mm	0.080 (–0.041 to 0.198)	0.19
RCA_ref	0.104 (–0.016 to 0.221)	0.09
RCA_6mm	0.096 (–0.024 to 0.214)	0.12
LAD_2mm	0.140 (0.020 to 0.256)	0.02
LAD_ref	0.148 (0.028 to 0.263)	0.02
LAD_6mm	0.147 (0.027 to 0.262)	0.02
LCX_2mm	0.160 (0.041 to 0.275)	0.009
LCX_ref	0.170 (0.051 to 0.285)	0.005
LCX_6mm	0.141 (0.021 to 0.257)	0.02

ACS, acute coronary syndrome; RCA, right coronary artery; LAD, left anterior descending artery; FAI, fat attenuation index; LCX, left circumflex artery; RCA_2mm, FAI around the proximal RCA within a 2-mm diameter from the outer vessel wall; RCA_ref, FAI around the proximal RCA within reference diameter from the outer vessel wall; RCA_6mm, FAI around the proximal RCA within a 6-mm diameter from the outer vessel wall; LAD_2mm, FAI around the proximal LAD within a 2-mm diameter from the outer vessel wall; LAD_ref, FAI around the proximal LAD within reference diameter from the outer vessel wall; LAD_6mm, FAI around the proximal LAD within a 6-mm diameter from the outer vessel wall; LCX_2mm, FAI around the proximal LCX within a 2-mm diameter from the outer vessel wall; LCX_ref, FAI around the proximal LCX within reference diameter from the outer vessel wall; LCX_6mm, FAI around the proximal LCX within a 6-mm diameter from the outer vessel wall.

Table S3 Logistic regression analysis of risk factors and PCAT attenuation in the proximal coronary associated with ACS

Characteristic	Univariable			Multivariable		
	OR	95% CI	P	OR	95% CI	P
Age	1.04	1.00–1.07	0.03	1.04	1.00–1.08	0.03
Gender						
0	Reference					
1	1.04	0.57–1.93	0.89	–	–	–
BMI	1.04	0.94–1.15	0.42	–	–	–
Obesity						
0	Reference					
1	1.22	0.54–2.77	0.63	–	–	–
Smoking						
0	Reference					
1	1.24	0.66–2.35	0.51	–	–	–
Drinking						
0	Reference					
1	1.02	0.45–2.36	0.95	–	–	–
Diabetes						
0	Reference					
1	1.15	0.59–2.24	0.68	–	–	–
Dyslipidemia						
0	Reference			Reference		
1	1.71	0.93–3.17	0.09	1.87	0.95–3.72	0.07
Family history						
0	Reference					
1	0.00	0.00–Inf	0.99	–	–	–
Hypertension						
0	Reference			Reference		
1	1.63	0.50–5.28	0.41	0.92	0.26–3.56	0.90
2	1.63	0.64–4.14	0.30	1.15	0.41–3.35	0.79
3	2.24	1.12–4.51	0.02	1.32	0.60–2.87	0.49
FAI around proximal coronary						
LAD_2mm	1.01	0.98–1.05	0.38	–	–	–
LAD_ref	1.03	1.00–1.07	0.05	1.02	0.95–1.09	0.60
LAD_6mm	1.03	1.00–1.07	0.09	1.02	0.95–1.09	0.59
LCX_2mm	1.00	0.97–1.04	0.86	–	–	–
LCX_ref	1.01	0.98–1.04	0.57	–	–	–

Table S3 (continued)

Table S3 (continued)

Characteristic	Univariable			Multivariable		
	OR	95% CI	P	OR	95% CI	P
LCX_6mm	1.02	0.98–1.05	0.33	–	–	–
RCA_2mm	1.01	0.98–1.04	0.65	–	–	–
RCA_ref	1.01	0.98–1.04	0.36	–	–	–
RCA_6mm	1.01	0.98–1.05	0.36	–	–	–
Gensini score	1.03	1.02–1.05	<0.001	1.03	1.02–1.05	<0.001

PCAT, pericoronary adipose tissue; OR, odds ratio; 95%CI, 95% confidence interval; BMI, body mass index; FAI, fat attenuation index; FAI, fat attenuation index; LCX, left circumflex artery; RCA_2mm, FAI around the proximal RCA within a 2-mm diameter from the outer vessel wall; RCA_ref, FAI around the proximal RCA within reference diameter from the outer vessel wall; RCA_6mm, FAI around the proximal RCA within a 6-mm diameter from the outer vessel wall; LAD_2mm, FAI around the proximal LAD within a 2-mm diameter from the outer vessel wall; LAD_ref, FAI around the proximal LAD within reference diameter from the outer vessel wall; LAD_6mm, FAI around the proximal LAD within a 6-mm diameter from the outer vessel wall; LCX_2mm, FAI around the proximal LCX within a 2-mm diameter from the outer vessel wall; LCX_ref, FAI around the proximal LCX within reference diameter from the outer vessel wall; LCX_6mm, FAI around the proximal LCX within a 6-mm diameter from the outer vessel wall.

References

37. Williams B, Mancia G, Spiering W, Agabiti Rosei E, Azizi M, Burnier M, Clement DL, Coca A, de Simone G, Dominiczak A, Kahan T, Mahfoud F, Redon J, Ruilope L, Zanchetti A, Kerins M, Kjeldsen SE, Kreutz R, Laurent S, Lip GYH, McManus R, Narkiewicz K, Ruschitzka F, Schmieder RE, Shlyakhto E, Tsioufis C, Aboyans V, Desormais I. 2018 ESC/ESH Guidelines for the management of arterial hypertension. *Eur Heart J* 2018;39:3021-104.
38. Jacobson TA, Ito MK, Maki KC, Orringer CE, Bays HE, Jones PH, McKenney JM, Grundy SM, Gill EA, Wild RA, Wilson DP, Brown WV. National lipid association recommendations for patient-centered management of dyslipidemia: part 1--full report. *J Clin Lipidol* 2015;9:129-69.
39. 2. Classification and Diagnosis of Diabetes: Standards of Medical Care in Diabetes-2020. *Diabetes Care* 2020;43:S14-s31.
40. Liu R, Gao X, Liang S, Zhao H. Five-years' prognostic analysis for coronary artery ectasia patients with coronary atherosclerosis: A retrospective cohort study. *Front Cardiovasc Med* 2022;9:950291.